http://dx.doi.org/10.1590/1678-4162-13145

Arq. Bras. Med. Vet. Zootec., v.76, n.2, p.207-216, 2024

Detoxification of groundwater pollutants from Al Jifara plain (Libya) using naturally synthesized chitosan: Histological and antioxidant status in Wistar Rats

[*Desintoxicação de poluentes de águas subterrâneas da planície de Al Jifara (Líbia) usando quitosana sintetizada naturalmente: status histológico e antioxidante em ratos Wistar*]

H.A.E. *Absisah*, W.S. *Hasheesh*, H.A. *Mohamed*, A.A. *Abdel-Khalek*[*]

Department of Zoology, Faculty of Science, Cairo University, Giza, Egypt

ABSTRACT

To evaluate the efficiency of naturally derived chitosan as a bio-adsorbent to improve water quality in Jefara plain and health condition, male Wistar rats divided into 7 groups: group I (drinking unpolluted water), group II (drinking untreated water from aquifer 1), group III (drinking water from aquifer 1 treated with 0.5gm/L chitosan), group IV (drinking water from aquifer 1 treated with 1 gm/L chitosan), group V (drinking with untreated water from aquifer 2), group VI (drinking water from aquifer 2 treated with 0.5gm/L chitosan, group VII (drinking water from aquifer 2 treated with 1 gm/L chitosan) for 30 days. Adsorptive ability of chitosan was confirmed by X-ray diffraction, scanning electron microscopy with energy dispersive X-ray after the exposure processes. The recorded antioxidant biomarkers showed marked elevations superoxide dismutase, glutathione reduced and thiobarbituric acid reactive substances levels in groups II and V. The application of chitosan, significantly ($P< 0.05$) reduced the TBARS level compared to untreated groups indicating the improvement of antioxidant status. Severity of structural damages of all recorded alterations in renal and hepatic tissues was more pronounced in the rats groups that were exposed to untreated water. While, chitosan intervention is significantly reduced the above recorded alterations.

Keywords: groundwater, chitosan, histopathology, antioxidant

RESUMO

Com o objetivo de avaliar a eficiência de quitosana naturalmente derivada como bio-absorvente para melhorar a qualidade da água e condições de saúde em Jefara, ratos Winstar machos foram divididos em 7 grupos: grupo I (bebendo água não poluída), grupo II (bebendo água não tratada do aquífero 1), grupo III (bebendo água do aquífero 1 tratada com 5gm/L de quitosana), grupo IV (bebendo água do aquífero 1 tratada com 1gm/L de quitosana), grupo V (bebendo água não tratada do aquífero 2), grupo VI (bebendo água do aquífero 2 tratada com 0,5 gm/L de quitosana, grupo VII (bebendo água do aquífero 2 tratada com 1gm/L de quitosana) por 30 dias. A capacidade de adsorção da quitosana foi confirmada por difração de raios X, microscopia eletrônica de varredura com dispersão de energia de raios X após os processos de exposição. Os biomarcadores antioxidantes registrados mostraram elevações acentuadas dos níveis de superóxido dismutase, glutationa reduzida e substâncias reativas ao ácido tiobarbitúrico nos grupos II e V. A aplicação de quitosana reduziu significativamente ($P<0,05$) o nível de TBARS em comparação com os grupos não tratados, indicando a melhoria do status antioxidante. A gravidade dos danos estruturais de todas as alterações registradas nos tecidos renal e hepático foi mais pronunciada nos grupos de ratos que foram expostos à água não tratada. Por outro lado, a intervenção da quitosana reduziu significativamente as alterações registradas acima.

Palavras-chave: água subterrânea, quitosana, hitopatologia, antioxidante

*Corresponding author: ecoamr@gmail.com, ecoamr@cu.edu.eg
Submitted: September 7, 2023. Accepted: November 7, 2023.

INTRODUCTION

In developing countries, clean drinking water is a major issue. Almost 800 million people worldwide lack access to safer drinking water sources, with 84% of this population living in developing countries (Bridget *et al*., 2023). Each year, approximately 2 million people die from diarrheal diseases caused by contaminated water supply and sanitation, with most of them being children under the age of five in developing countries (WHO & UNICEF, 2015). Libya is an arid region, and it is one of the North African countries experiencing severe water shortages because of the country's rapid development. Libya has experienced a severe water scarcity due to the lack of permanent rivers and the erratic nature of its rainfall. The northern aquifers of the Jefara plain are the most important renewable aquifer system in Tripoli which recharged naturally from rainfall infiltrating directly or through wadis. In many locations, groundwater has become contaminated due to infiltration of contaminated surface water, raising the degree of contamination in relation to the hydrologic characteristics of the aquifers, weather patterns, disposal method, quantity, and toxicity of wastes (Alfarrah and Walraevens, 2018). In addition, excessive water pumping may deteriorate purity of the groundwater due to the influx of more mineralized water from covering strata to the well and causing seawater to migrate inland and start rising toward the wells (Shailaja and Johnson, 2007). Among the seventeen sustainable development goals (SDGs), providing access to clean water ranks sixth. Therefore, water management, planning, and conservation are the key issues in coastal parts of Jefara Plain. Fundamentally, contamination of groundwater can be caused by anthropogenic and/or natural processes. The most common contaminants identified in groundwater of Jefara Plain are metals, minerals, ammonia sulphate, nitrates and nitrites. To resolve these problems, researchers have focused their efforts on developing treatment and disposal methods for toxic pollutants such as nanofiltration, chemical precipitation and biosorption (Fouda *et al*., 2022). Biopolymers maintain their dominance over all the other manufactured polymeric substances because they are more environmentally friendly. Aranaz *et al*. (2009) described chitosan as a natural polymer made of glucosamine and Nacetyl glucosamine copolymers that can be obtained by partial deacetylation of chitin (the main structural component of shrimp and crab shells). In the present study, the adsorption properties of naturally extracted chitosan is used against several pollutants in two contaminated groundwater wells from Jefara plain, Libya.

In this regard, the present approach aimed to evaluate the efficiency of naturally derived chitosan as a bio-adsorbent to improve water quality in Jefara plain and health condition of male Wistar rat (*Rattus norvegicus*) using integrated physicochemical, antioxidant, and histological endpoints.

MATERIALS AND METHODS

Study areas. Site 1: Samples were collected from groundwater wells with an average depth of 280 meters in the Sidi Al-Saih area in the northern Jaffara Plain. It is one of the suburbs south of the city of Tripoli, the Libyan capital, which contains the largest concentration of population in the country. Sidi Al-Saih is about 47 kilometers from the center of the capital, and it contains a high population density in addition to the agricultural activity in the region. Groundwater of the area is drawn from dug wells which are essential for drinking, domestic use and agricultural purposes. GPS: E32°52, N13°29. Site 2: Samples were collected from groundwater wells in the Tiji area with an average depth of 120 meters, southwest of the Jafara Plain. The city of Tiji is about 250 km southwest of the capital, Tripoli, and contains a medium population density in addition to the medium agricultural activity in the region. GPS: E 32°041, N 11°42.

Water sampling was done based on the standard methods for the examination of water and wastewater according to APHA (2017). Water samples (n=3) were obtained from each site in polyethylene containers. For metal analysis, concentrated nitric acid was added to reduce the pH of the collected samples (below 2) to prevent any microbial reactions. As described by Sauter and Stoup (1990), NH_3 was determined colorimetrically using Nessler's solution. All recorded cations and anions concentrations in water samples were measured by ion chromatography (IC) (model DX-600, USA) according to APHA (2017). The concentrations

of eight metals were estimated in water samples according to (APHA, 2017) using inductively coupled plasma (ICP-AES), Thermo Sci, model: iCAP6000 series. Procedure blanks were sucked in addition to the measuring process to correct background absorption to evaluate the measurement process' accuracy. Additionally, standard reference material (Lake Superior fish 1946 NIST, National Institute of Standards and Technology, USA) was used and the metal recovery ranges were between 93 % and 103 %.

Chitosan preparation. Wet samples of 10 g of chopped shrimp shells were weighed and then oven-dried for 4 days at 65°C to obtain a constant weight. Then the shrimp exoskeletons were boiled in 500mL beakers containing (2% w/v) sodium hydroxide (NaOH) for 1 h to remove the protein content from the shrimp shell. Cool for 30 min at room temperature. The treated shrimp shells were powdered to obtain size ranging from 0.5 to 5.0mm using a meat tenderizer. Shell powder was further soaked in 1% HCl with four times its quantity for 24 h to remove the minerals from shells. The processed shrimp shell powder was treated with 50 mL of a 2% sodium hydroxide solution for about 1 h to decompose the albumen into water soluble fractions. The obtained chitin was thoroughly washed with milli-Q water and the supernatant was totally removed. The obtained chitin was boiled in 50% NaOH for 2 h at 100°C. The samples were allowed to cool down at room temperature. The samples were washed repeatedly with 50% NaOH followed by filtration to obtain the solid chitosan. The samples were dried in hot air oven at 110°C for 6 h to obtain creamy-white powder.

Characterization of synthesized chitosan. To investigate the structure of the synthesized chitosan to verify the chemical composition, size, shape, crystal structure and surface charge, X-ray diffraction (XRD), scanning electron microscopy (SEM) with energy dispersive X-ray (EDX), and zeta potential (ZP) were determined. The sizes of the resulting particles were then determined using Scherrer's equation. All size and morphological information on the produced powder was provided by SEM and XRD techniques. Using the entire ICCD PDF-2 database file, the GBC X-ray analysis TRACES Program (Version 6) was used to do the minerals analysis. Malvern Zeta Sizer Nano ZS instrument is used to deliver full surface charge information.

Two concentrations of chitosan were selected as low (0.5gm/L) and high (1gm/L) concentrations to detect the most proper concentration to remove the highest amount of all studied contaminants from water (Fig. 1).

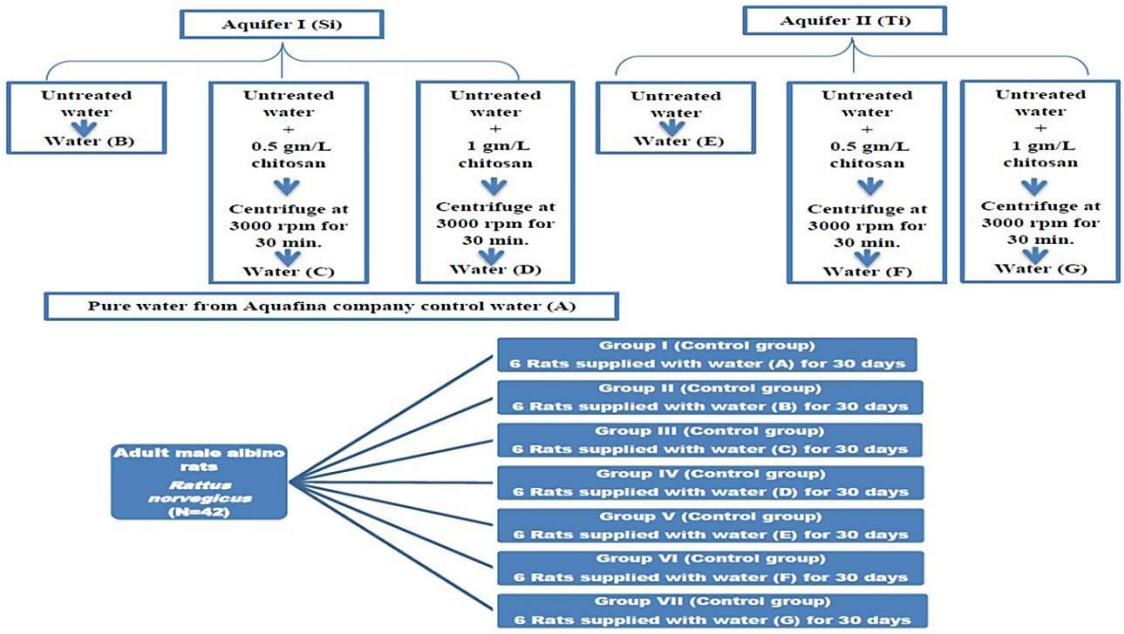

Figure 1. The experimental design.

The oxidative biomarkers. oxidative status within kidneys, and livers was evaluated by measuring the enzymatic activities of superoxide dismutase (U/mg proteins). The total protein in the studied tissues was measured as described by Ardry (1960). The superoxide dismutase (SOD) activities were determined colorimetrically (at 560 nm) according to Nishikimi *et al*. (1972), who relied on the inhibition rate of SOD for the phenazine methosulphate-mediated reduction of nitroblue tetrazolium dye. The levels of GSH were determined according to the methods described by Rahman *et al*. (2006). The content of thiobarbituric acid reactive substances (TBARS) was measured in the studied tissues (nmole/g tissue) as an indicative sign of lipid peroxidation degree. Thiobarbituric acid can react with malondialdehyde in an acidic medium at 95°C to form TBARS. TBARS content was estimated colorimetrically at 534 nm after pink color formation (Ohkawa *et al*., 1979).

Histopathological analysis. Isolated tissues (Kidneys and livers) were rinsed in 0.9% saline many times before being preserved in Bouin's fixative. As described by Bernet *et al*. (2001), samples were paraffin sectioned at 4 µm and stained with hematoxylin and eosin (H and E stain).

Statistical analysis. Statistical Processor Systems Support, SPSS software, version 16.0, IBM, Chicago, IL, USA, was used to analyze data. The data were presented as the mean and standard error. The raw data were normally distributed as tested by the Shapiro–Wilk, and Kolmogorov–Smirnov tests and homogeneous as shown by Levene's test. To determine the comparability between all investigated groups, data were statistically analyzed using analyses of variance ANOVA test and Duncan's multiple ranges as represented by different letters at a significant level of $p<0.01$.

RESULTS

Characterization of synthesized chitosan. As shown in Fig. 2A, the diffraction peaks of synthesized chitosan at 2θ values of 11.321°, 14.064°, 15.530°, 16.425°, 21.287°, 29.323°, 31.399°, 33.212°, 36.137°, 38.213°, 39.736°, 42.208°, 47.873°, 48.822°, 50.681°, 51.996°, 52.555°, 53.886°, 55.530°, 56.341°, 61.508°, 63.753°, 67.030°. Different mineral phases of calcium carbonate in the form of mineral calcite in addition to traces of Coesite (SiO_2). The crystalline size was valued to be 43.28 ± 7.74 µm using Scherrer's formula. Fig. 2B showed that the synthesized particles are on the micro-scale with irregular shapes. The zeta potential -0.08mV.

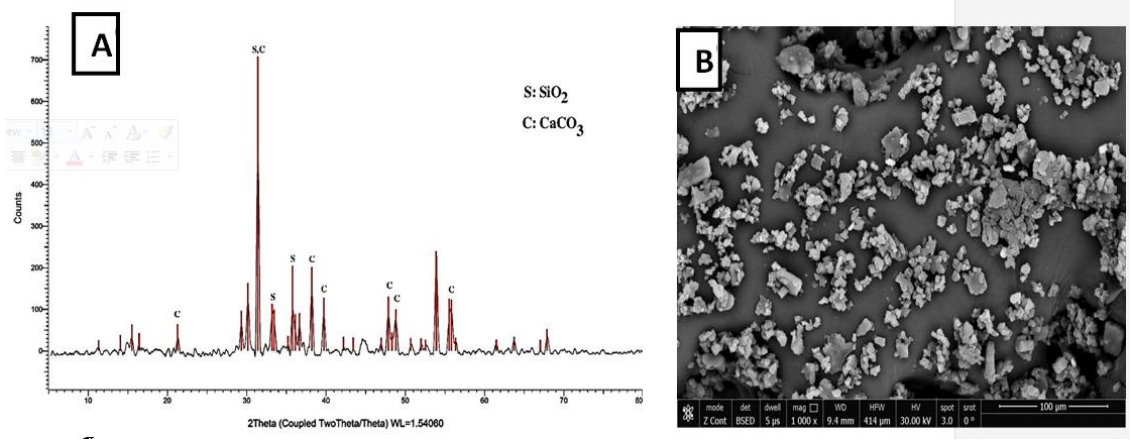

Figure 2. X-ray diffraction (XRD) and scanning electron microscopy (SEM) of the synthesized chitosan.

Analysis of metals and undesirable substances. The levels of ammonium, nitrate, nitrite, phosphate, silica, Fe, Mn, Cu, Zn, CN, Pb, Cd, Al in water are detailed in Table 1. All recorded parameters showed various degrees of contamination with significant elevations in group II followed by group V. Chitosan- treated groups showed a marked decrease in all recorded parameters compared to untreated groups.

Table 1. Analysis of metals and undesirable substances

Groups	Ammonium	Nitrate	Nitrite	Phosphate	Silica	Fe	Mn	Cu	Zn	CN	Pb	Cd	Al
Group I	0.0A	0.094A	0.0A	0.076A	0.0A	0.017A	0.024A	0.467A	0.274A	0.0A	0.0003A	0.0A	0.0006A
	±0.0	±0.0034	±0.0	±0.001	±0.0	±0.004	±0.0035	±0.018	±0.0147	±0.0	±0.00033	±0.0	±0.00033
Group II	1.54D	4.62C	1.32D	0.286E	0.396B	1.815D	0.495F	3.179D	1.815E	0.165F	0.067E	0.042E	0.032F
	±0.081	±0.242	±0.069	±0.015	±0.021	±0.095	±0.026	±0.166	±0.095	±0.009	±0.0035	±0.002	±0.0016
Group III	1.065B	0.355A	0.278BC	0.144B	0.317B	1.219B	0.2016B	1.968B	1.190B	0.038B	0.0221B	0.017B	0.014B
	±0.0256	±0.0085	±0.0067	±0.0034	±0.0076	±0.029	±0.0048	±0.047	±0.0286	±0.0009	±0.0005	±0.00042	±0.00035
Group IV	1.242C	0.514B	0.349C	0.194C	0.339B	1.367C	0.349D	2.240C	1.367C	0.087D	0.039C	0.026C	0.017CD
	±0.022	±0.009	±0.006	±0.0034	±0.006	±0.0244	±0.0062	±0.040	±0.0244	±0.0015	±0.0007	±0.0004	±0.0003
Group V	1.156BC	0.568B	0.333C	0.245D	6.713C	1.489C	0.401E	2.371C	1.509D	0.137E	0.05D	0.029D	0.021E
	±0.0136	±0.006	±0.0039	±0.003	±0.079	±0.017	±0.005	±0.027	±0.017	±0.0016	±0.0006	±0.0003	±0.0002
Group VI	1.072B	0.407B	0.228B	0.208C	0.337B	1.361C	0.288C	2.265C	1.361C	0.069C	0.041C	0.026CD	0.015BC
	±0.004	±0.0015	±0.0008	±0.0007	±0.0012	±0.005	±0.001	±0.008	±0.005	±0.0002	±0.0001	±0.0001	±0.00006
Group VII	1.094B	0.439B	0.312B	0.205C	0.361B	1.397C	0.361D	2.266C	1.445CD	0.087D	0.042C	0.028CD	0.018DE
	±0.0148	±0.0059	±0.0042	±0.0027	±0.0049	±0.018	±0.0049	±0.031	±0.019	±0.0011	±0.0005	±0.0003	±0.0002
F value	199.900	304.816	252.694	121.393	6073.44	201.799	204.974	137.735	142.772	265.647	225.853	212.387	183.434
P value	<0.05	<0.05	<0.05	<0.05	<0.05	<0.05	<0.05	<0.05	<0.05	<0.05	<0.05	<0.05	<0.05

- Data are represented as means of three samples in each group ± S.E.
- The capital letters represent Duncan's test ($p < 0.05$) among different groups. Columns with the same capital letters are not significantly different; otherwise, they do.
- The letters are arranged in Ascending order as A, B, C, and D.

Energy-dispersive X-ray spectroscopy. The data obtained from energy-dispersive X-ray spectroscopy (Fig. 3), confirmed the existence of different metals and minerals on the surfaces of synthesized chitosan. As demonstrated in Fig. 3A, the surface analysis and imaging of free synthesized chitosan showed that the major surface components are carbon and oxygen with traces of Cu, Zn, and K. The application of synthesized chitosan (low concentrations; Fig 3B) confirmed the presence of Na, Mg, Al, Br, Si, P, Cl, Fe, Cu, Ca on the surfaces of chitosan particles. While the application of high concentration of chitosan (Fig. 3C) showed the existence of Al, Si, Zn on the surfaces.

Antioxidant biomarkers in kidney and liver tissues. Fig. 4 and 5 show the activity of SOD in addition to GSH and TBARS levels in the kidneys and livers of the studied groups, respectively. In kidneys, content of GSH were elevated in group II and IV compared to other groups. Chitosan-treated groups showed marked decline in GSH content compared to untreated groups (except for high concentration group of aquifer one; group IV). The activities of SOD in the groups representing aquifer one showed significant elevation compared to aquifer two. While the activities of SOD were declined after chitosan treatment of all studied groups. Significant elevations in TBARS content were observed after exposure to untreated water of both aquifers. However, the application of chitosan (low and high concentrations) significantly reduced the level of TBARS compared to untreated groups. In liver, same results were recorded except for insignificant increase of SOD after chitosan treatment in aquifer two (groups VI and VII).

Histopathological analysis. The histological structures of the studied renal and hepatic tissues are represented in Fig. 6 and 7, respectively.

Kidney. Renal architecture in the control rats was observed to be normal with universally shaped renal tubules (RT) with regular hematopoietic tissues between them. In rats administered untreated water, the renal tissue showed widened Bowman's space (W) with shrunken glomeruli (S), infiltration of red blood cells (IF), intra-luminal exfoliation of epithelial cells (IE), vascular congestion (C). Additionally, glomerular capillary congestion and severe renal tubule necrosis with obvious irregularities in their basement membranes were seen.

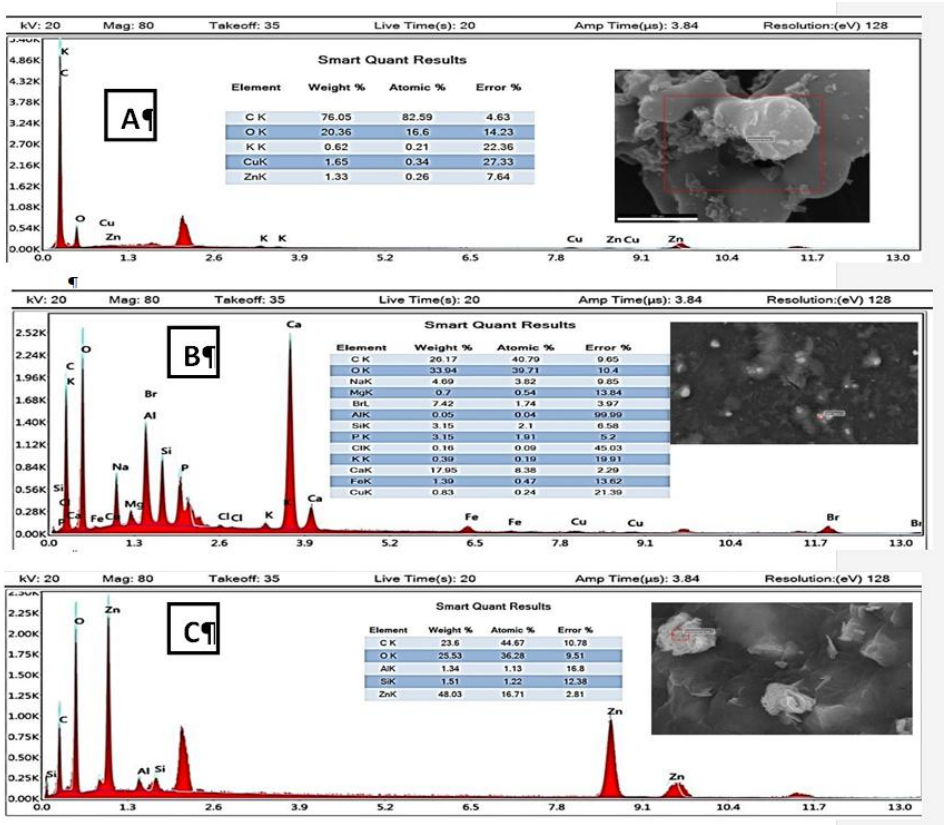

A: free chitosan; B: Low concentration chitosan after exposure to untreated water; C: high concentration chitosan after exposure to untreated water.

Figure 3. Energy dispersive X-ray (EDX) of the synthesized chitosan.

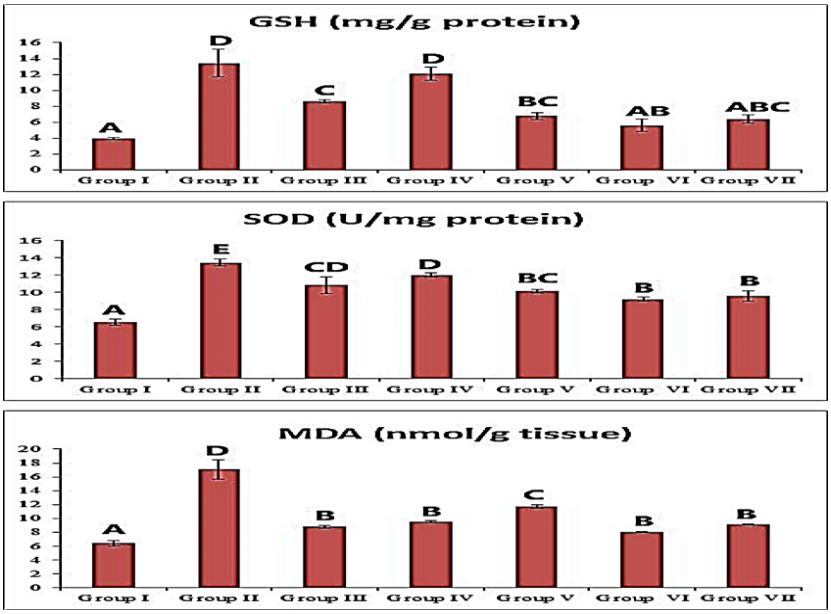

- Data are represented as means of six samples in each group ± S.E.
- The capital letters represent Duncan's test ($p < 0.05$) among different groups. Columns with the same capital letters are not significantly different; otherwise, they do.
- The letters are arranged in Ascending order as A, B, C, and D.

Figure 4. Antioxidant biomarkers in kidney of Wistar rats of the studied groups.

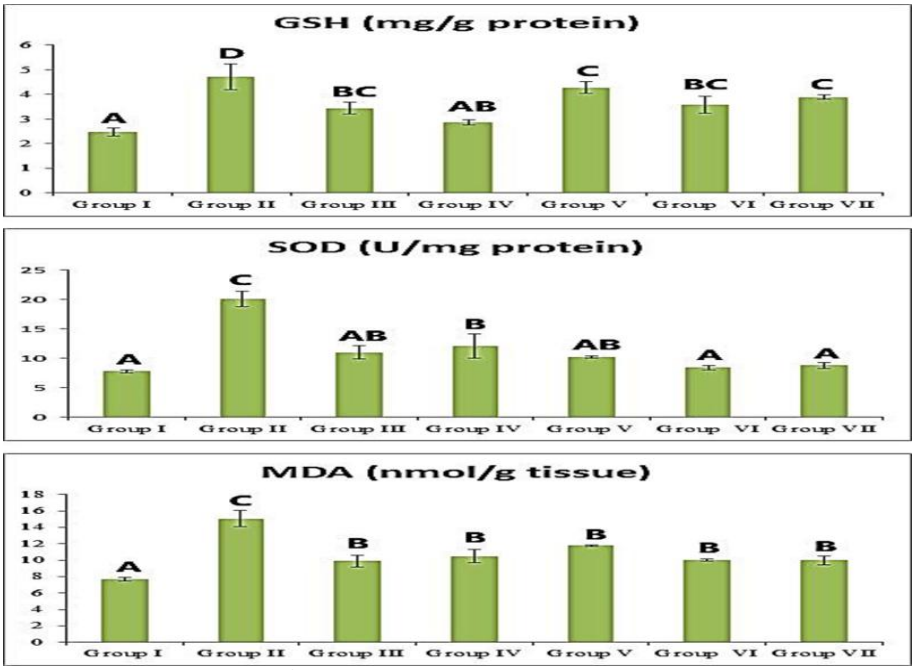

- Data are represented as means of six samples in each group ± S.E.
- The capital letters represent Duncan's test ($p < 0.05$) among different groups. Columns with the same capital letters are not significantly different; otherwise, they do.
- The letters are arranged in Ascending order as A, B, C, and D.

Figure 5. Antioxidant biomarkers in liver of Wistar rats of the studied groups.

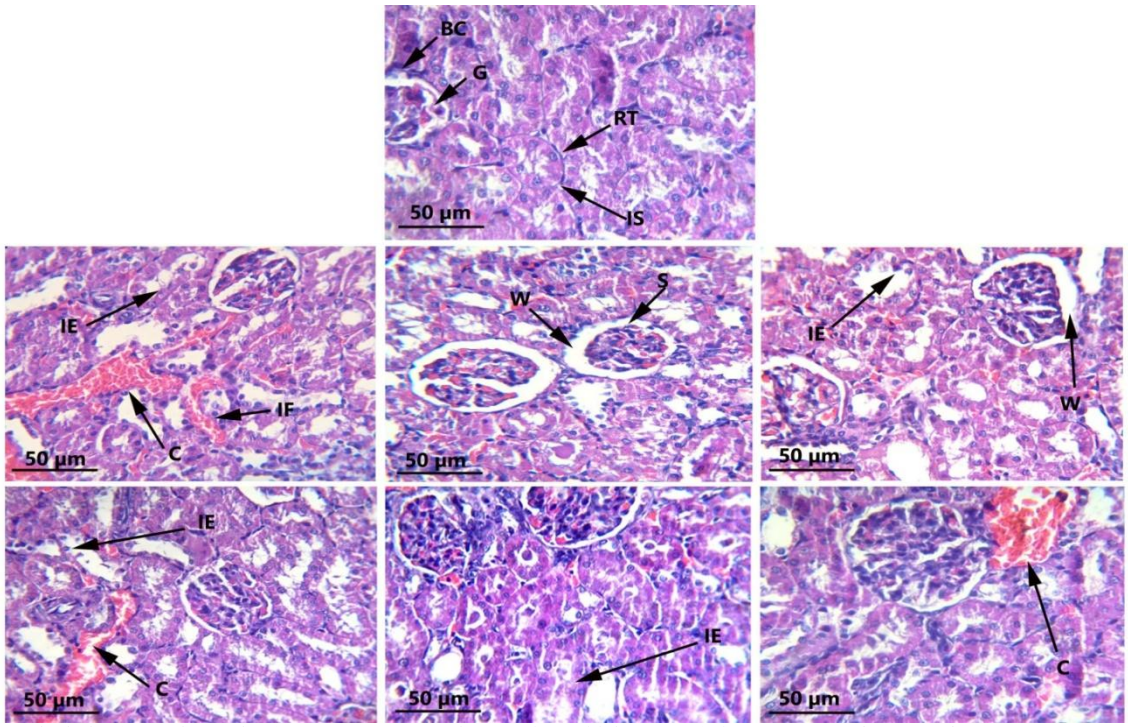

Renal tubules (RT); glomerulus (G); Bowman's capsule (BC); interstitial space (IS); intra-luminal exfoliation of epithelial cells (IE); Infiltration of blood cells (IF); Blood congestion (C) Shrinkage in glomerulus (S); widening of Bowman's space (BS).

Figure 6. Representative histopathological alterations in renal tissues of the studied groups.

Liver. The normal histological structure of hepatocytes (H) was recorded in the hepatic tissues of the control rats, with normal central or sub-central spherical nuclei and homogeneous cytoplasm. Whereas liver sections of rats exposed to untreated water (groups II and V) showed marked deteriorations in liver architecture as degeneration in hepatocytes (D); intense peri-portal inflammatory (I) with infiltration of blood cells (IF); melanomacrophage aggregation; cytoplasmic vacuolization (V), slight dilatation of the portal vein (D).

Generally, the severity of the structural damages based on the frequency of alterations appearance and the size of affected area of all recorded alterations was more pronounced in the rat groups that were exposed to untreated water especially from aquifer one. While chitosan intervention is significantly reduced the above recorded histological alterations.

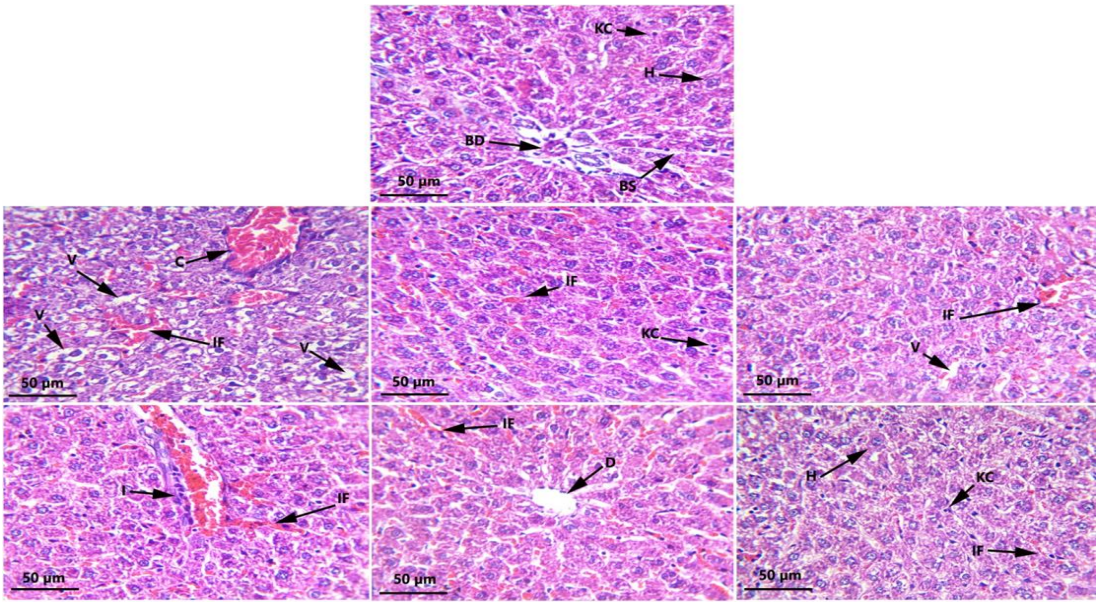

Hepatocytes (H); Blood sinusoids (BS); Bile duct (BD); Kupffer cells (KC); Infiltration of blood cells (IF); Vacuolization (V); Blood congestion (C); intense peri-portal inflammatory cellular infiltration (I); dilatation of the portal vein (D).

Figure 7. Representative histopathological alterations in hepatic tissues of the studied groups.

DISCUSSION

The supply of clean water is now a major global concern as water is becoming incredibly limited (Jamei *et al.*, 2022). Drinking water accessibility, food and energy security, and biological community are all impacted by the groundwater budget. Fundamentally, contamination of groundwater can be caused by anthropogenic and/or natural processes. The present data showed the toxicological impacts of untreated groundwater in Libya on the antioxidant status and histological structures of the studied animal model. Therefore, drinking groundwater should be treated before use. In this context, the goal of the current study was to elucidate adsorption behavior of naturally synthesized chitosan against several undesirable pollutants in water. After chitosan- water treatment, improvements were seen in all water parameters as well as the examined oxidative stress and histological biomarkers. This improvement is consistent with the study's hypothesis suggesting the efficiency of chitosan in eliminating different kinds of aquatic pollutants. Many methods have been used to remove pollutants from water, including chemical precipitation, nanofiltration and biosorption (Fouda *et al*., 2022). Chitosan is a high molecular weight, linear cationic polymer that is biodegradable and non-toxic (El Knidri *et al*., 2018). Chitosan is a substance that can be employed as adsorbents due to its unique chemical composition and physical characteristics. Considering that the amine group ($-NH_2$) and hydroxyl group (-OH) on the polymer chain of chitosan can adsorb both

cationic and anionic compounds, therefore chitosan is frequently used to get rid of heavy, transition metals, and other pollutants from wastewaters (Chatterjee *et al*., 2009). The efficient adsorption ability may also be due to the greater number of pores in the surface of chitosan particles. Besides, due to reverse surface charge, an overdose of chitosan results in somewhat lower removal efficiency when the amount of chitosan used is greater than the saturation points for polymer bridging, the remaining chitosan breaks down the polymer bridge between the particles and the residual amount of chitosan. Additionally, as polymer adsorption increases the polymer's charge density will increase and the quick destabilization of the particles will occur (Ariffin *et al*., 2005). That is why the efficiency of low dose chitosan in the present study to absorb more minerals and metals was higher than the high dose. As represented by EDX and removal % results, the effectiveness of chitosan particles showed maximum levels at low dose treatment compared with the high dose. Rats have a powerful enzymatic antioxidant defense system to protect cells from several toxic oxygen species (Beloucif *et al*., 2021). Oxidative stress is a significant factor in toxicity. It is accepted to be a consequence of increased production of free radicals and reactive oxygen species (ROS), and/ or decrease in antioxidant defense. The increasing trend in SOD in group II could be due to the remarkably increased H_2O_2 accumulation in rats that depend on untreated water as water source. Javed *et al*. (2016) reported that frequent and chronic exposure to metal pollution speeds up the formation of GS-metal complexes by increasing the rate at which metals bind to GSH (through its thiolate sulfur atom). Particularly, the elevated GSH and SOD do not appear to be very protective at scavenging all ROS generated in excess, potentially causing lipid peroxidation indirectly. The relatively low GSH level and SOD activities following natural chitosan NPs intervention may be responsible for their role in oxidative stress overcome, as evidenced by the low TBARS level. Water treatment by chitosan succeeded in decreasing the concentration of many undesirable substances in addition to decrease metal toxicity via adsorption of several metals and decreasing their bioavailability. Aside from antioxidant enzymes, TBARS content has been identified as a reliable measure of membrane damage (Ghosh *et al*., 2016). The current study found that chitosan intervention reduced TBARS levels significantly, indicating less membrane injury. Using untreated groundwater resulted in several histopathological changes, including infiltration of red blood cells, intra-luminal exfoliation of epithelial cells, and vascular congestion in renal tissues in addition to degeneration in hepatocytes, peri-portal inflammation, and cytoplasmic vacuolization in hepatic tissues. The elevated level of metallothioneins (MTs) generation in kidney and liver cells, which progressively develops a chelate with metals to avoid potential harm, maximized the xenobiotic-renal cells and hepatocyte interaction (Moussa *et al*., 2022). Red blood cells occupying renal and hepatic interstitial spaces suggests that cellular membrane structural integrity has been lost. According to Mahboob *et al*. (2020), these alterations are frequently related to a prolonged necrotic state. Vacuolization degeneration was linked by Ciji and Nandan (2014) to either excessive cytoplasmic fat deposition or the imbalance between the rates of material production and consumption by hepatocytes. According to Lee *et al*. (2015), excess lipids accumulation could be an indication of oxidative injury. The increase of inflammatory cells linked to metal pollution may be the cause of the necrotic degeneration and tubular distortion (Abdel-Khalek *et al*., 2020).

CONCLUSION

In general, the rats that were exposed to untreated groundwater had more severe structural damage, especially from aquifer II, as showed by frequent appearance of documented alterations. Therefore, due to chemical and physical properties of naturally synthesized chitosan particles, they can be successively treated and converted into efficient biosorbents.

REFERENCES

ABDEL-KHALEK, A.; BADRAN, R.; MARIE, M. The efficient role of rice husk in reducing the toxicity of iron and aluminum oxides nanoparticles in *Oreochromis Niloticus*: hematological, bioaccumulation, and histological endpoints. Water Air Soil Pollut., v.231, p.1-15, 2020.

ALFARRAH, N.; WALRAEVENS, K. Groundwater overexploitation and seawater intrusion in coastal areas of arid and semi-arid regions. *Water*, 10, p.2-10, 2018.

ARANAZ, I.; MENGÍBAR, M.; HARRIS, R. *et al*. Functional characterisation of chitin and chitosan. *Curr. Chem. Biol*., v.3, p.203-230, 2009.

ARDRY, R. The determination of proteins by the biuret reaction. Determination of a specific absorption coefficient. *Ann. Biol. Clin*., v.18, p.214-222, 1960.

ARIFFIN, A.; SHATAT, R.; NIK NORULAINI, A.; MOHD OMAR, A. Synthetic polyelectrolytes of varying charge densities but similar molar mass based on acrylamide and their applications on palm oil mill effluent treatment. *Desalination*, v.173, p.201-208, 2005.

BELOUCIF, A.; KECHRID, Z.; BEKADA, A.M.A. Effect of zinc deficiency on blood glucose, lipid profile, and antioxidant status in streptozotocin diabetic rats and the potential role of sesame oil. *Biol. Trace Elem. Res*., v.200, p.3236-3247, 2021.

BERNET, D.; SCHMIDT, H.; MEIER, W.; BURKHARDT-HOLM, P.; WAHLI, T. Histopathology in fish: proposal for a protocol to assess aquatic pollution. *J. Fish. Dis*., v.22, p.25-34, 2001.

BRIDGET, S.; FAKHREDDINE, S.; RATEB, A. *et al*. Global water resources and the role of groundwater in a resilient water future. *Nat. Rev. Earth Environ*., v.4, p.87-101, 2023.

CHATTERJEE, T.; CHATTERJEE, S.; NOO, S. Enhanced coagulation of bentonite particles in water by a modified chitosan biopolymer. *Chem. Eng. J*., v.148, p.414-419, 2009.

CIJI, P.; NANDAN, S. Toxicity of copper and zinc to *Puntius parrah* (Day, 1865). *Mar. Environ. Res*., v.93, p.38-46, 2014.

EL KNIDRI, H.; BELAABED, R.; ADDAOU, A.; LAAJEB, A.; LAHSINI, A. Extraction, chemical modification and characterization of chitin and chitosan. *Int. J. Biol. Macromol*., v.120, p.1181-1189, 2018.

FOUDA, A.; EID, M.; EL-BELELY, F. *et al*. Enhanced antimicrobial, cytotoxicity, larvicidal, and repellence activities of phyco-synthesized magnesium oxide nanoparticles using brown algae, cystoseira crinita. *Fronte. Bioeng. Biotechnol*., v.28, p.849-921, 2022.

GHOSH, S.; SHAW, K.; AZAHAR, I. *et al*. Arsenate (AsV) stress response in maize (Zea mays L.). *Environ. Exp. Bot*., v.130, p.53-67, 2016.

JAMEI, M.; KARBASI, M.; MALIK, A. *et al*. Computational assessment of groundwater salinity distribution within coastal multi-aquifers of Bangladesh. *Sci. Rep*., v.12, p.11165, 2022.

JAVED, M.; AHMAD, I.; USMANI, N.; AHMAD M. Studies on biomarkers of oxidative stress and associated genotoxicity and histopathology in *Channa Punctatus* from heavy metal polluted canal. *ChemoSphere*, v.151, p.210-219, 2016.

LEE, J.; HOMMA, T.; KURAHASHI, T.; KANG, E.; FUJII, J. Oxidative stress triggers lipid droplet accumulation in primary cultured hepatocytes by activating fatty acid synthesis. *Biochem. Biophysiol. Res. Commun*., v.14, p.229-235, 2015.

MAHBOOB, S.; KHALID, A.; AL-GHANIM, H. *et al*. Toxicological effects of heavy metals on histological alterations in various organs in Nile tilapia (*Oreochromis niloticus*) from freshwater reservoir. *J. King Saud Univ. Sci*., v.32, p.970-973, 2020.

MOUSSA, M.; MOHAMED, H.; ABDEL-KHALEK, A. The antioxidant defense capacities and histological alterations in the livers and gills of two fish species, *Oreochromis Niloticus* and *Clarias Gariepinus*, as indicative signs of the batts drain pollution. *Environ. Sci. Pollut. Res*., v.29, p.71731-71741, 2022

NISHIKIMI. M.; APPAJI, N.; YAGI, K. The occurrence of superoxide anion in the reaction of reduced phenazine methosulfate and molecular oxygen. *Biochem. Biophysiol. Res. Commun*., v.46, p.849-854, 1972.

OHKAWA, H.; OHISHI, N.; YAGI, K. Assay for lipid peroxides in animal tissues by thiobarbituric acid reaction. *Anal. Biochem*., v.95, p.351-358, 1979.

RAHMAN, I.; KODE, A.; BISWAS, S.K. Assay for quantitative determination of glutathione and glutathione disulfide levels using enzymatic recycling method. *Nat. Protoc*., v.1, p.3159-3165, 2006.

SAUTER, A.; STOUP, K. Waters and Salt. In: Helrich, K., Ed., AOAC Official Methods of Analysis (15th Edition), Association of Official Analytical Chemists (AOAC), Arlington, Virginia, 1298 p, 1990

SHAILAJA, K.; JOHNSON, M. Fluorides in groundwater and its impact on health. *J. Environ. Biol*., v.28, p.331-332, 2007.

STANDARD methods for the examination of water and wastewater. 23.ed. Washington, D.C.: APHA, 2017.

WHO (World Health Organization) & UNICEFF (United Nations International Children's Emergency Fund). 25 Years Progress on Sanitation and Drinking water 2015 Update and MDG Assessment. Geneva, Switzerland: WHO Press., 2015.